Nanoscale Research Letters
a SpringerOpen Journal

NANO EXPRESS Open Access

A facile approach to synthesize $SiO_2 \cdot Re_2O_3$ (Re = Y, Eu, La, Sm, Tb, Pr) hollow sphere and its application in drug release

Zhihua Li[1*], Lin Zhu[1], Qian Liu[1], Yu Du[1] and Feng Wang[2]

Abstract

Multifunctional $SiO_2 \cdot Re_2O_3$ (Re = Y, Eu, La, Sm, Tb, Pr) hollow spheres (HSs) have been fabricated using an acidic Re^{3+} ion solution. Under ultraviolet radiation, functional HSs emit different colors of light according to the different rare-earth ions embedded into the shell of SiO_2 hollow spheres. The as-prepared hollow capsules were characterized by X-ray diffraction, transmission electron microscopy, high-resolution transmission electron microscopy, Brunauer-Emmett-Teller method, scanning electron microscopy, and energy-dispersive spectrometry. Drug loading and release experiments have been carried out using $SiO_2 \cdot Eu_2O_3$ HSs that acted as drug carriers. The results demonstrate that the multifunctional HSs exhibit a high storage capacity and the ability of retaining drug stability and activity, which indicates that the as-synthesized fluorescent hollow capsules are a potential candidate as drug delivery materials.

Keywords: $SiO_2 \cdot Re_2O_3$; Hollow spheres (HSs); Fluorescence

Background

Recently, much attention have been focused on the research of hollow SiO_2 spheres (HSSs) because of their excellent properties such as thermal stability, large surface areas, low density, low toxicity, and good compatibilities with other materials [1-15]. So, HSSs have attracted intense interest and have been widely applied in a variety of fields, such as catalysis, sensors, chromatography, dyes, inks, photonic crystals, cells, waste removal, shield for enzymes or proteins, delivery vehicle of drugs, and large biomolecular release [16-28]. In general, three approaches are employed to prepare HSSs: template methods [6,29-31], self-assembly technique, and microemulsions [32,33]. HSSs [34-36] have been fabricated with the soft template and hard template methods, which involve complicated procedures such as shell formation and core removal. The template-free method has attracted much attention due to its simple and economical characteristic [27,28]. In 2008, Zhang et al. [25] developed a self-template method to convert solid silica into hollow spheres (HSs). In the process, silica is dissolved into $NaBH_4$ solution and silicate species deposited on the surface of the silica colloid. The shell formed over the silicate species via Ostwald ripening results in HSSs. An alkalescent environment is an inevitable synthesis condition that is reported in nearly all papers [37-50]; the only exception is that of Chen et al. who used HF as an etching agent [51]. In 2011, Wang's group reported firstly the synthesis of HSSs in generic acidic media [52]. Unfortunately, the published work was based on the study of only two factors: pH value and Na^+ ion, which influence the formation process of HSSs.

Herein, we report a one-step self-driven process to synthesize multifunctional HSSs under an acidic condition with rare-earth ion assistance. Compared with Wang's report, the synthetic approach of HSSs is simpler. Being synthesized with the assistance of rare-earth ions, the as-prepared HSSs can emit bright fluorescence under ultraviolet radiation, which is convenient to be detected in real time if it is used in biological applications. Typical drug loading and release experiments are carried out using our prepared multifunctional HSSs, $SiO_2 \cdot Eu_2O_3$ HSs.

* Correspondence: lizhihua2006@126.com
[1]Department of Chemistry, College of Chemistry, Chemical Engineering and Materials Science, Shandong Normal University, Jinan 250014, China
Full list of author information is available at the end of the article

Methods

All chemicals were of analytical grade and purchased from Jinan Camolai Trading Company (Jinan, China), which were used as received without further purification: tetraethyl orthosilicate (TEOS, 98%), ammonium hydroxide solution ($NH_3 \cdot H_2O$, approximately 25% in water), nitric acid (HNO_3, 65%), Re_2O_3, and ethanol (C_2H_5OH). Rare-earth nitrate solutions [$Re(NO_3)_3$ (Re = Y, Eu, La, Sm, Tb, Pr)] with a concentration of 0.04 to 0.08 mol/L were prepared by ourselves.

Synthesis of monodisperse silica spheres

Silica spheres with a diameter of 200 to 500 nm were prepared by the hydrolysis of TEOS in the mixture of ethanol, water, and ammonium using the Stöber process [37-39].

Synthesis of $SiO_2 \cdot Re_2O_3$ hollow spheres

In a typical synthesis, silica spheres (0.06 g) were added to 20 mL $Re(NO_3)_3$ (0.06 mol/L) and stirred for 30 min. The pH of the solution is 4.5 (adjusted with dilute nitric acid). The mixture was transferred into a Teflon-lined stainless autoclave (capacity 25 mL) and heated at 250°C for 12 h. After the products naturally cooled down to room temperature, they were washed with deionized water and separated by centrifugation (4,000 rpm) for three times and then dried at 60°C for 4 h in the air.

Drug storage and release

The steps of drug storage and release are as follows:

1. $SiO_2 \cdot Eu_2O_3$ HSs (1 g) were added into a 50-mL hexane solution containing 40 mg/mL ibuprofen (IBU). The mixture was sealed and stirred for 24 h. Then the sample was separated by centrifugation and dried at 60°C in the air. The filter was characterized by UV-visible (UV–vis; 264 nm) spectroscopy.
2. The dry $SiO_2 \cdot Eu_2O_3$ loaded with IBU (0.1 g) was immersed into 50 mL of simulated body fluid (SBF; pH = 7.4) at 37°C and stirred at the rate of 100 rpm. Three milliliters from the top of the solution was used for release measurement at different intervals, and then 3 mL of fresh SBF is added into the solution to keep the volume unchanged.

Characterization and instruments

The characterization and instruments used are detailed as follows:

1. The samples were characterized by X-ray diffraction (XRD) with a Philips X'Pert Super diffractometer (Amsterdam, The Netherlands) with graphite-monochromatized Cu Kα radiation (λ = 1.54178 Å) in the 2θ range of 1.5° to 10° and 10° to 80°.
2. The transmission electron microscopy (TEM) images and electron diffraction (ED) patterns were obtained using a Hitachi 800 transmission electron microscope (Chiyoda-ku, Japan) with an accelerating voltage of 200 kV.
3. The high-resolution transmission electron microscopy (HRTEM) images were obtained using JEOL-2010 (Akishima-shi, Japan).
4. The UV–vis absorption spectra of the samples were measured using a UV-1800 ultraviolet–visible spectrophotometer (Shanghai Meipuda Instrument Co., Ltd., Shanghai, China).

The samples used for characterization were ultrasonically dispersed in absolute ethanol for 30 min before the TEM and HRTEM tests.

Results and discussion

Characterization of $SiO_2 \cdot Eu_2O_3$ HSs

Newly prepared silica spheres were used to fabricate HSSs. The monodispersed SiO_2 spheres with an average diameter of 230 nm (Figure 1A) were fabricated using the Stöber method [37-39] and acted as the template. The hollow $SiO_2 \cdot Eu_2O_3$ HSs were uniform, as shown in the HRTEM image in Figure 1B, whose size was nearly unchanged. XRD curves in Figure 1C demonstrate that both the SiO_2 sphere and $SiO_2 \cdot Eu_2O_3$ hollow sphere are amorphous (compared with ICSD #174). The absence of diffraction peaks for Eu_2O_3 was owing to the few content of Eu_2O_3 in the sample. Figure 2 shows the HRTEM image and energy-dispersive spectrometer (EDS) analysis of $SiO_2 \cdot Eu_2O_3$ HSs. A large number of holes with different sizes on the surface of $SiO_2 \cdot Eu_2O_3$ HSs could be observed in Figure 2A, which belonged to a range of mesoporous structures according to the diameter of holes. The $SiO_2 \cdot Eu_2O_3$ HSs with numerous mesoporous structures indicated that they are potential drug carriers for application in medicine, e.g., targeting therapy. The results of the EDS analysis showed that the content of O, Si, and Eu was 72.43%, 25.15%, and 2.22%, respectively. The microcontent of Ge (0.19%) was due to the impurity coming from the reagent of Eu_2O_3. The SiO_2 HSs were amorphous according to their XRD pattern, so the lattice fringe that appeared on the HRTEM image (Figure 2B) stemmed from Eu_2O_3. The measured interplanar spacing of 0.3 nm corresponded to the (001) plane of Eu_2O_3. Obviously, Eu_2O_3 is one component of the final product, and it may be embedded into the shells or form a kind of composite similar to 'alloy' or a solid solution. Further research is in progress. Being doped with Eu_2O_3 on the surface of SiO_2 HSs, the obtained samples can emit bright red light under an ultraviolet beam. HRTEM observation also revealed that the HSs produced in the solution contained Re^{3+}

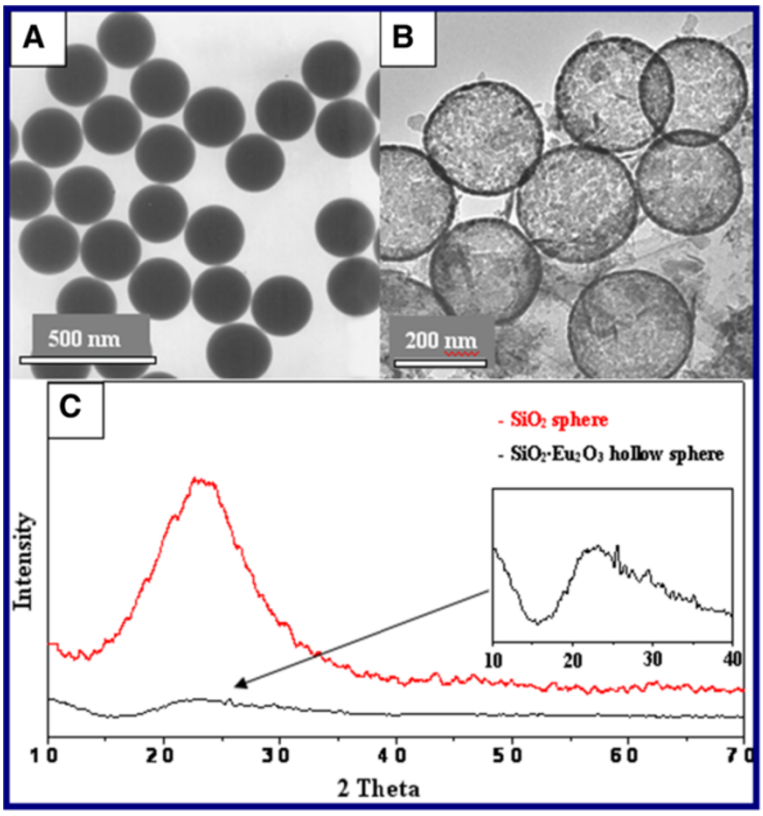

Figure 1 TEM image of SiO_2 sphere (A), HRTEM image of $SiO_2 \cdot Eu_2O_3$ HSs (B), XRD patterns of SiO_2 sphere and $SiO_2 \cdot Eu_2O_3$ HSs (C). The insert is magnification of one segment of XRD.

ions that formed a mesoporous structure with different orientations.

The measured emission spectrum curve of $SiO_2 \cdot Eu_2O_3$ HSs is shown in Figure 3. The strong red emission peak further suggested that Eu^{3+} existed in the surface of the SiO_2 hollow sphere. The emission spectrum of $SiO_2 \cdot Eu_2O_3$ HSs consisted of peaks mainly located in the wavelength range from 570 to 700 nm. These peaks corresponded to transitions from the excited state $^5D_0$ to the ground state ^7F_J ($J = 0, 1, 2, 3, 4$) of the $4f^6$ configuration of Eu^{3+}, as marked in Figure 3. Luminescence originating from transitions between $4f$ levels is predominant due to electric dipole or magnetic dipole interactions [40-44]. As can be seen in Figure 3, the strong red emission peak at 612 nm originating from the electric dipole transition $^5D_0$ to $^7F_2$ was the dominant band in the measured spectrum. The emission peak at around 590 nm was attributed to the $^5D_0$ to $^7F_1$ transition. The peaks located at 648 and 695 nm corresponded to $^5D_0$ to $^7F_3$ and $^5D_0$ to $^7F_4$ transitions, respectively.

Figure 4 shows the Brunauer-Emmett-Teller (BET) N_2 adsorption-desorption isotherms and the pore size distribution of the as-prepared $SiO_2 \cdot Eu_2O_3$ HSs. The BET specific surface area and the total pore volume of the $SiO_2 \cdot Eu_2O_3$ HSs were measured to be 308.6 m^2/g and 0.307 cm^3/g, respectively. The pore diameter distribution was relatively wide according to the data of the adsorption branch of the isotherm. The as-prepared $SiO_2 \cdot Eu_2O_3$ HSs with a mesoporous structure may possess good performance in drug delivery efficiency, catalytic activity, and so on.

Influencing factors of the synthetic process of $SiO_2 \cdot Re_2O_3$ (Re = Y, Eu, La, Sm, Tb, Pr) hollow structures

The experiments showed that the pH value of the solution, reaction temperature and time, and different rare-earth ions and concentrations played an outstanding role in the synthesis of $SiO_2 \cdot Re_2O_3$ hollow structures, which are discussed in detail as follows.

Effect of the pH value of the solution

The pH value of the solution was adjusted with dilute nitric acid. The studied pH range was from 7 to 3 under the following reaction conditions: $Re^{3+} = 0.06$ mol/L and $T = 250$°C. Hollow-structure particles could be obtained under the range of $4 \le pH < 5.5$, and the optimum pH value was 4.5. No hollow structure products appeared when $6 \le pH \le 8$. No HSSs appeared when $2 < pH < 3$. Normally, a few HSSs could have emerged in the product at the conditions of $3 < pH < 4.0$ or $5 < pH < 6$ if the

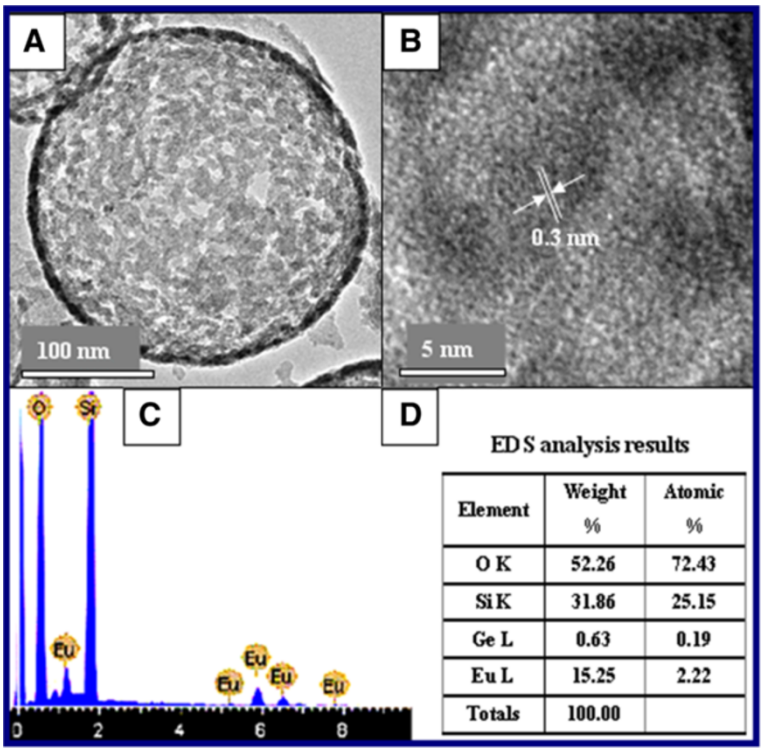

Element	Weight %	Atomic %
O K	52.26	72.43
Si K	31.86	25.15
Ge L	0.63	0.19
Eu L	15.25	2.22
Totals	100.00	

Figure 2 HRTEM images and EDS pattern of $SiO_2 \cdot Eu_2O_3$ HSs. (A) Mesoporous structure of $SiO_2 \cdot Eu_2O_3$. **(B)** The interplanar spacing of the (001) plane of Eu_2O_3. **(C, D)** EDS pattern and results of $SiO_2 \cdot Eu_2O_3$ HSs, respectively.

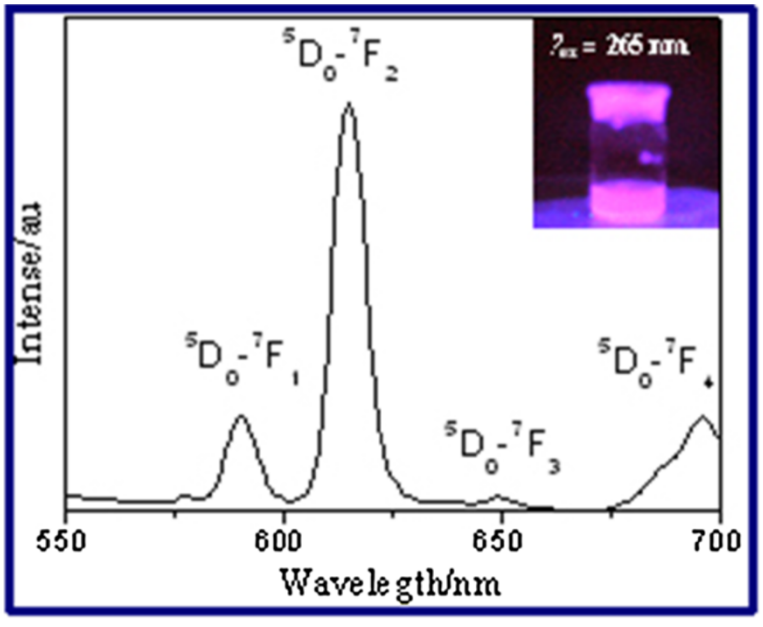

Figure 3 The emission spectrum of SiO_2·Eu_2O_3 HSs. The insert is digital image of SiO_2·Eu_2O_3 HSs under UV light.

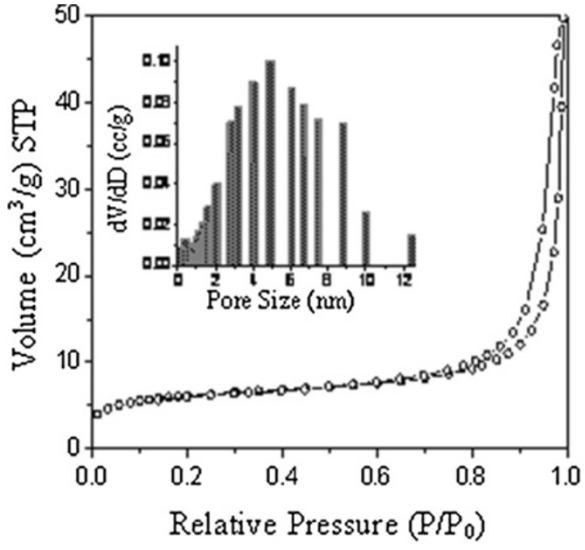

Figure 4 N_2 adsorption-desorption isotherm and pore size distribution (insert) of SiO_2·Eu_2O_3 HSs.

reaction time was more than 10 h. The detailed results are shown in Additional file 1: Table S1 and Figure S3. It is known that SiO_2 is an amphoteric oxide which can dissolve into an acidic or basic solvent. The experiments showed that a weak acid solution was in favor of hollow structure formation. The experiments also revealed that the experimental results were unaffected when using other acids such as HCl or H_2SO_4 to adjust the pH value of the solution.

Effect of reaction temperature

The temperature of the hydrothermal reaction affected greatly not only the reaction (going or not) but also the reaction rate (slow or fast). Additional file 1: Figure S1 shows the TEM images of the as-prepared samples at different reaction temperatures. No hollow-structure products appeared if the temperature $T < 230$°C in our experiments. The morphology and size of nanocrystals became difficult to control when the temperature was up to 260°C or higher because the higher the temperature was, the faster the reaction rate was. When $T = 255$°C, the quality of the obtained $SiO_2 \cdot Re_2O_3$ HSs was always poor. The experiments verify that the moderate temperature was 250°C.

Effect of Re^{3+} ion and its concentration

It was reported that Na_2SO_4 and NaCl were advantageous to HSS formation [52] and the work matter was Na^+ cation, which was in line with our experimental data. Hereby, we investigated the synthesis of HSSs under different rare-earth ions and bivalent cations.

In order to get uniform hollow structures, the optimal concentration of the rare-earth ions was usually kept in the range of 0.04 to 0.08 mol/L. The experimental data and TEM images are depicted in Additional file 1: Table S1 and Figure S2. The concentration less than 0.03 mol/L resulted in poor quality in production, and the concentration greater than 0.08 mol/L always led to products with not all having a hollow structure. The experiments showed that the lower or higher concentration of Re^{3+} ions was not good for HSS formation and 0.06 mol/L was the optimal concentration.

Although the $SiO_2 \cdot Re_2O_3$ HSs were obtained based on the rare-earth ion assistance strategy, their quality was quite different under assistance of different kinds of rare-earth ions. By keeping other reaction conditions unchanged such as the pH value of the solution, reaction time, and reaction temperature, the influence of different Re^{3+} ions (Re = Y, Eu, La, Sm, Tb, Pr) on the structure of the as-prepared products was investigated (see Additional file 1: Table S2 and Figure S4). Additional file 1: Figure S4 clearly shows that the influence sequence of Re^{3+} was as follows: $Eu^{3+} \approx Sm^{3+} > Y^{3+} > Pr^{3+} \approx La^{3+} > Tb^{3+}$. Nearly all of the as-prepared samples were hollow spheres with good quality under the effect of Eu^{3+} and Sm^{3+} existence, and the experiments showed good reproducibility and satisfactory results. With Y^{3+}, Pr^{3+}, and La^{3+} ions included, all of the products always formed a mixture of HSSs and core/shell structure. Furthermore, all of the samples can be formed into a hollow sphere if the reaction time is prolonged, but the yield of HSSs was lower. Only a small amount of HSs could be obtained with Tb^{3+} existence. The experiments indicated that changing the reaction time did not work.

We compared the synthesis approach under the same reaction conditions using Mg^{2+}, Ca^{2+}, Mn^{2+}, Zn^{2+}, and Cu^{2+} instead of Re^{3+} ions. The results showed that $SiO_2 \cdot$ HSs could barely be obtained at the above situations, which indicated that rare-earth ion was an indispensable factor in hollow structure formation.

Experimental data showed that the rare-earth ions were advantageous to HSS formation; however, further study is needed to understand why the effect of different Re^{3+} ions on the formation of HSSs has a different role.

Effect of reaction time

The reaction time will determine the deepening of the reaction after fixing other reaction conditions. Figure 5 shows the structures of the as-prepared particles with a variety of reaction time. As can be seen, rattle-type particles appeared after 6 h of reaction, and then the core of particles gradually disappeared and finally became HSs at about 8 h, meanwhile many tiny particles accompanied with the HSs. After 10 h, the shapes of HSs were clearer, though many tiny particles were around them. The tiny particles came from the dissolved SiO_2, which

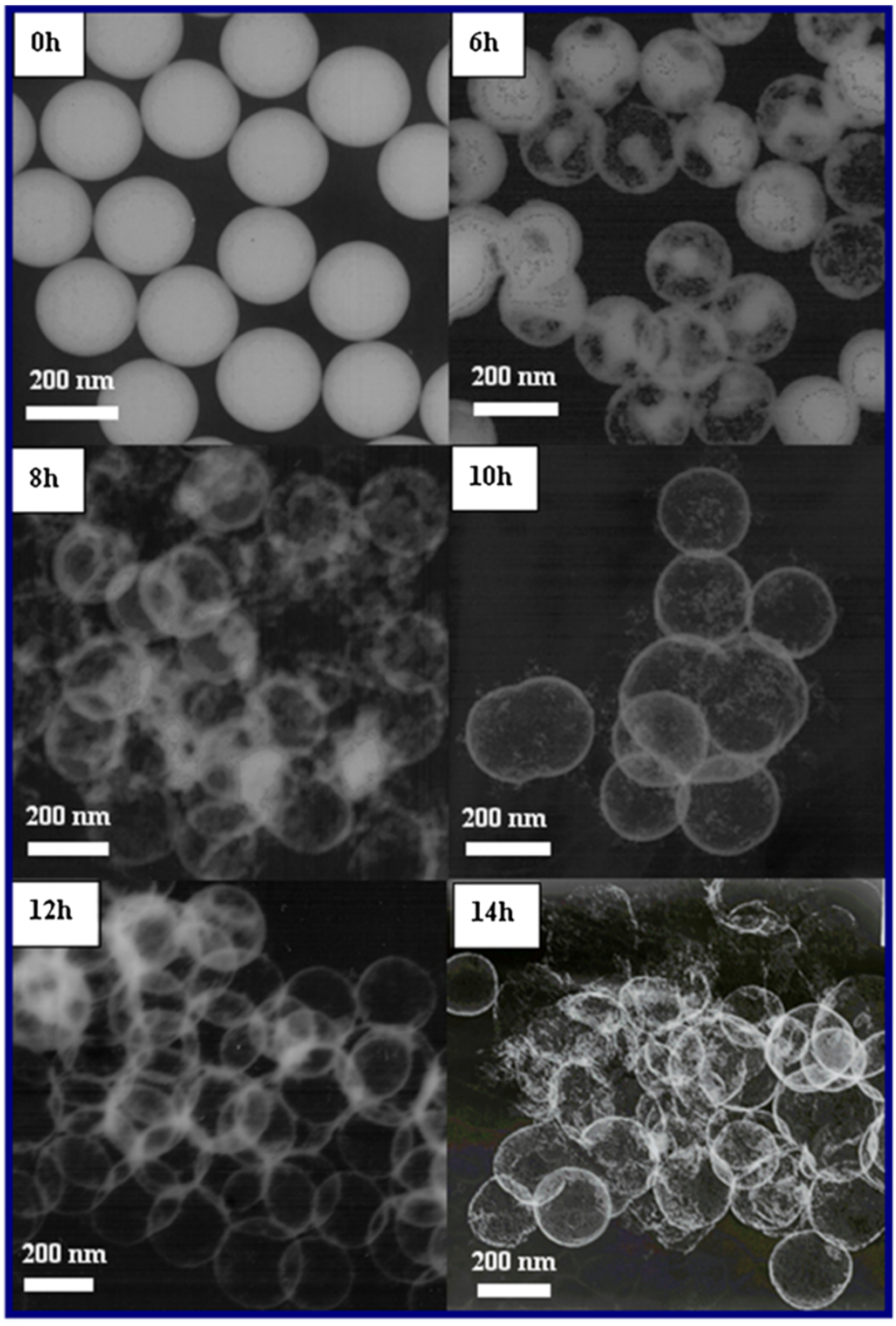

Figure 5 TEM images of products prepared at different reaction time. T = 250°C, pH = 4,[Eu^{3+}] =0.06 mol/L.

disappeared with reaction time extension. The high-quality HSs with clear edges were obtained when the reaction lasted for 12 h; simultaneously, the tiny particles disappeared too. It was noticed that the shell of hollow spheres was getting thinner and thinner when the reaction time was over 12 h. As can be seen, a handful of HSs had cracked after 14 h. The experiments indicated that the reaction time would significantly vary the influence on the shell thickness of $SiO_2 \cdot Re_2O_3$ HSs. Therefore, the shell thickness of HSs can be controlled by adjusting the reaction time.

From the above, our synthesis procedure of HSSs is very simple and effective compared with those previously reported.

Formation mechanism of $SiO_2 \cdot Re_2O_3$ HSs

In our experiments, $SiO_2 \cdot Re_2O_3$ HSs were synthesized in an acidic solution. It was reported that colloid SiO_2 would carry a negative charge when pH > 3 [45]. The following equilibriums existed in the intermediate between the liquid and solid interfaces [48]:

$$SiO_2 \overset{H^+}{\leftrightarrow} HSiO_4^{3-} \overset{H^+}{\leftrightarrow} H_2SiO_4^{2-} \overset{H^+}{\leftrightarrow} H_3SiO_4^{-} \overset{H^+}{\leftrightarrow} H_4SiO_4 \overset{H^+}{\leftrightarrow} H_5SiO_4^{+} \cdots.$$

When Re^{3+} ions are added into the solution, an electrostatic force is produced between the surface of silica and Re^{3+}, Re^{3+} ions are absorbed onto the surface of SiO_2 spheres at first, and then insoluble compounds $SiO_2 \cdot Re_2O_3$ are formed. Meanwhile, SiO_2 cores keep dissolving in the acidic solution, as shown in Figure 5 (6 h). At the initial stage, most of the Re^{3+} ions are absorbed onto the surface of SiO_2 spheres, and numerous insoluble tiny particles that come from the residual Re^{3+} ions meet with the negative ions in the solution, as shown in Figure 5 (8 and 10 h). As the reaction continues, the tiny particles are swallowed by the $SiO_2 \cdot Re_2O_3$ lamella due to Ostwald ripening, and clear $SiO_2 \cdot Re_2O_3$ HSs are obtained at last, as shown in Figure 5 (12 h). Figure 6 is the sketch map of $SiO_2 \cdot Re_2O_3$ HS formation. In the first step, Re^{3+} would be adsorbed on the surface of the silica colloid, and then the silica colloid turns into a rattle-type particle and finally turns into a HS through Ostwald ripening after being treated in hydrothermal conditions.

The experiments showed that the diameter of $SiO_2 \cdot Re_2O_3$ HSs was almost the same as that of the template, which indicated that the size of $SiO_2 \cdot Re_2O_3$ HSs was determined by the SiO_2 solid spheres. Therefore, we can control the size of $SiO_2 \cdot Re_2O_3$ HSs by controlling the diameter of SiO_2 solid spheres.

Drug delivery and release

Considering that HSs have numerous mesoporous structures on the surface, they can act as drug loading capsules. IBU, a typical anti-inflammatory drug, is a good example used for drug loading experiments [49,53]. Herein, IBU was used to study the drug delivery and release behavior of nanostructured HSs.

The $SiO_2 \cdot Re_2O_3$ HSs were 1 g after loading IBU (see the 'Methods' section), and the IBU storage in nanostructured $SiO_2 \cdot Re_2O_3$ HSs reached 287.8 mg/g, which means that the as-prepared $SiO_2 \cdot Re_2O_3$ HSs have a high loading capacity.

The rate of drug release determines the drug effect. Slow and sustained drug release ensures a long drug effect. First of all, a phosphate buffer solution (PBS) of IBU (0.1 μg/mL) was prepared to find out the maximum absorption wavelength using a UV-visible spectrophotometer. The experiments indicated that the maximum absorption wavelength of IBU was 264 nm. According to the Lambert-Beer law, $A = kC$, where A is the absorbency, k is a constant, and C is the concentration of IBU in PBS. The insert of Figure 7A is the working curve of IBU in PBS, which was obtained by the measured absorbency of different PBS concentrations.

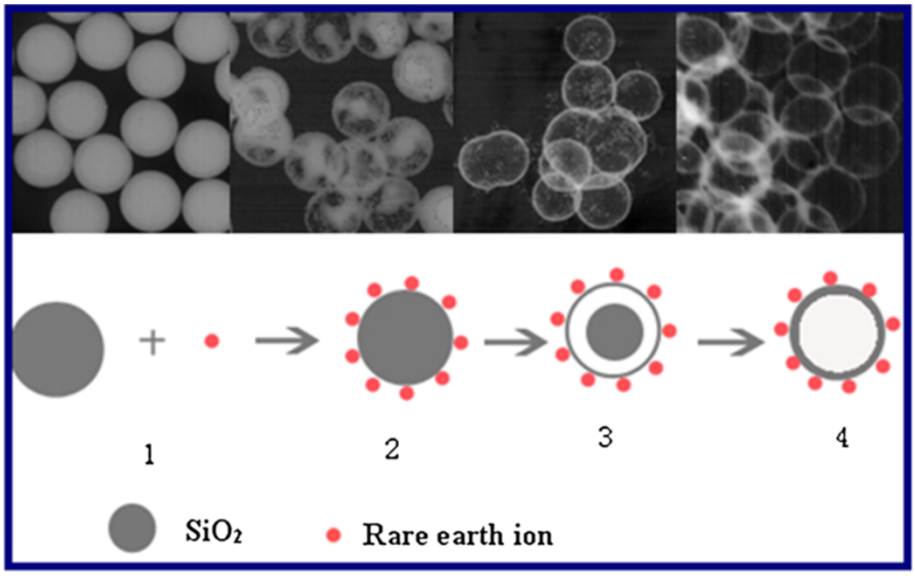

Figure 6 Schematic diagram of the formation of SiO_2·Re_2O_3 HSs.

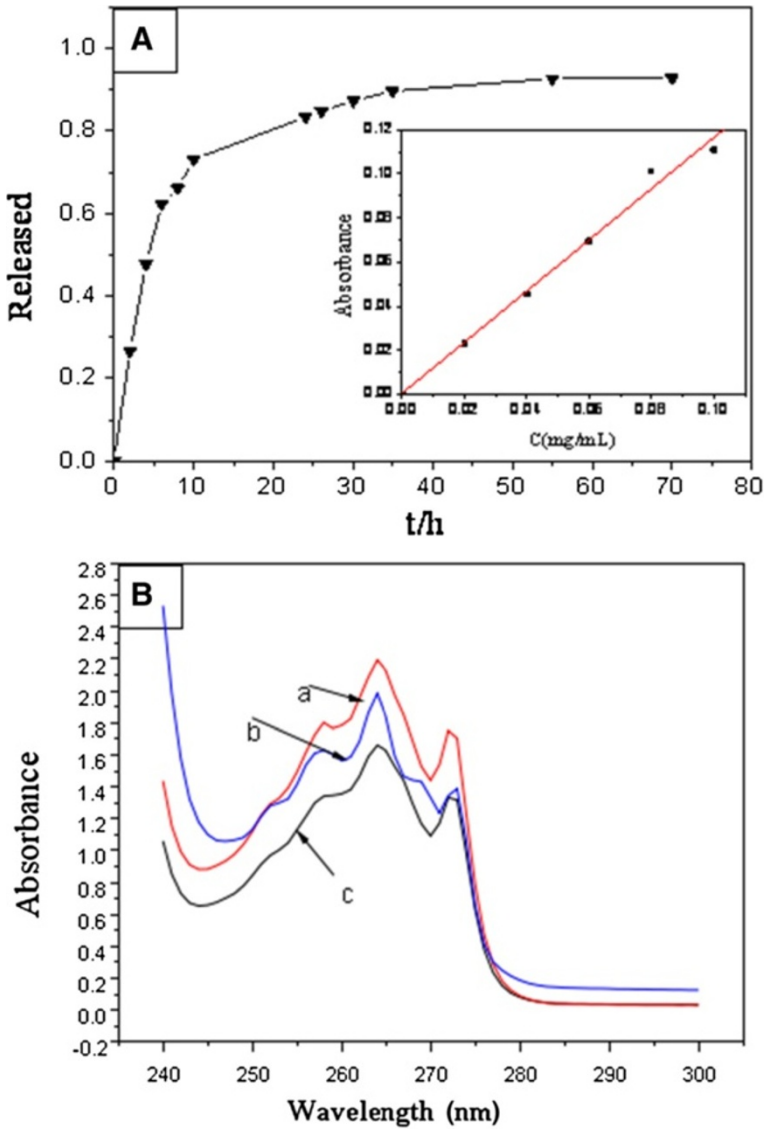

Figure 7 Release efficiency and UV–vis absorption spectra of IBU. (A) Release efficiency of IBU in the PBS system. The insert is the standard curve of CIBU absorbance. **(B)** The UV–vis absorption spectra of IBU in the different release times. Curve a, IBU hexane solution before drug loading; curve b, the SBF solution after the release of IBU-loaded $SiO_2 \cdot Eu2O_3$ HSs for 4 h; curve c, the SBF solution after the release of IBU-loaded $SiO_2 \cdot Eu_2O_3$ HSs for 70.

The relationship between the concentration of IBU in PBS and absorbency was as follows:

$$A = 1.14951C + 0.00109\ (\mathrm{mg/ml}),\ \text{its related coefficient}\ R^2 = 0.9948.$$

The released IBU concentration in SBF could be calculated using the following equation:

$$C = (A - 0.00109)/1.14915.$$

The total release rate of IBU can be calculated by the following equation:

$$\mathrm{R}(\%) = \frac{C_i * 50 + \sum_{1}^{i-1} C_i * 3}{m}$$

where R is the total release rate, C_i is the IBU concentration in SBF at time i, i is the time of the IBU medium solution taking out from the SBF, and m represents the total mass of the IBU in the HSs.

Figure 7A shows the release behavior of the IBU-loaded $SiO_2 \cdot Eu_2O_3$ HSs in SBF. Compared with the pure IBU disk release in SBF, the release rate of the IBU-loaded $SiO_2 \cdot Eu_2O_3$ HSs lasted long. The drug release rate was very fast within 12 h, which showed a nearly linear relationship between drug release rate and release time at the first 12 h. Then the drug release process was very slow and finished after 60 h. The results indicated that the sustained release behavior of the drug carrier was in favor of a durative drug effect.

In order to investigate the properties of the loaded drug, the UV–vis absorption spectra of the IBU hexane solution before and after IBU loading in $SiO_2 \cdot Eu_2O_3$ HSs were measured. The results are shown in Figure 7B. Curves a, b, and c were the IBU hexane solution before drug loading, the SBF solution after the release of IBU-loaded $SiO_2 \cdot Eu_2O_3$ HSs for 4 h, and the SBF solution after the release of IBU-loaded $SiO_2 \cdot Eu_2O_3$ HSs for 70 h, respectively. It was noticed that the shape of the absorption curves was essentially the same, which demonstrated that the property of IBU was not changed in the loading and release processes.

We noticed that the samples still emitted fluorescence after the experiments of drug delivery and release, which indicated that the leftover via the loading and release processes can be tracked and detected.

Conclusions

We have reported an approach of the synthesis of functional $SiO_2 \cdot Re_2O_3$ HSs using silica spheres, rare-earth ions, and an acidic environment. The size of synthesized hollow capsules can be modulated by controlling the diameter of the silica template. The facile and economical synthesis protocol is valuable and convenient for wide use. Acting as drug-loaded capsules, the $SiO_2 \cdot Re_2O_3$ HSs demonstrated much excellent properties of high payloads, retained drug activity and stability, and slow drug release rate. Furthermore, real-time detection may be carried out during drug delivery and release with $SiO_2 \cdot Re_2O_3$ HSs by measuring their fluorescence.

Additional file

Additional file 1: Supporting information. Table S1. Experimental results at different reaction conditions. **Table S2.** Different Re^{3+} ion (Re = Y, Eu, La, Sm, Tb, Pr) influence on the product during synthesis process. **Figure S1.** TEM images of different reaction temperatures, $[Eu^{3+}] = 0.06$ mol/L, 12 h. **Figure S2.** TEM images of different Eu^{3+} concentrations, 250°C, 12 h. **Figure S3.** TEM images of different pH values of solutions, 250°C, $[Eu^{3+}] = 0.06$ mol/L, 12 h. **Figure S4.** TEM images of $SiO_2 \cdot Re_2O_3$ HSs prepared by different Re^{3+} assistance: $T = 250$°C, pH = 4, $[Re^{3+}] = 0.06$ mol/L, $t = 12$ h (Re = Y, Eu, La, Sm, Tb, Pr).

Competing interests

The authors declare that they have no competing interests.

Authors' contributions

ZL is the director of the experiment group, who propounded the ideas and drafted the manuscript. LZ carried out the series of experiments and characterized all the samples. QL participated in the related experiments. YD participated in the experiment of drug loading and release. FW participated in its design and coordination. All authors read and approved the final manuscript.

Acknowledgements

The authors express their thanks to Associate Prof. Rusen Yang (University of Minnesota) for the language polishing.

Author details

[1]Department of Chemistry, College of Chemistry, Chemical Engineering and Materials Science, Shandong Normal University, Jinan 250014, China. [2]College of Rizhao Polytechnic, Rizhao 276826, China.

Received: 21 June 2013 Accepted: 27 September 2013
Published: 21 October 2013

References

1. Van Bommel KJC, Jung JH, Shinkai S: **Poly(L-lysine) aggregates as templates for the formation of hollow silica spheres.** *Adv Mater* 2001, **3**(19):1472–1476.
2. Fan WG, Gao LJ: **Synthesis of silica hollow spheres assisted by ultrasound.** *J Colloid Interf Sci* 2006, **297**(1):157–160.
3. Yeh YQ, Chen BC, Lin HP, Tang CY: **Synthesis of hollow silica spheres with mesostructured shell using cationic-anionic-neutral block copolymer ternary surfactants.** *Langmuir* 2006, **22**(1):6–9.
4. Zhu GS, Qiu SL, Terasaki O, Wei YJ: **Polystyrene bead-assisted self-assembly of microstructured silica hollow spheres in highly alkaline media.** *Am Chem Soc* 2001, **123**(31):7723–7724.
5. Caruso F: **Nanoengineering of particle surfaces.** *Adv Mater* 2001, **13:**11–22.
6. Tissot I, Reymond JP, Lefebvre F, Bourgeat-Lami E: **SiOH-functionalized polystyrene latexes. A step toward the synthesis of hollow silica nanoparticles.** *Chem Mater* 2002, **14:**1325–1331.
7. Liu SQ, Lu LC, Sui XY, Vera M, Pegie C, Etienne FV: **Fast fabrication of hollow silica spheres with thermally stable nanoporous shells.** *Microporous Mesoporous Mater* 2007, **98:**41–46.
8. Chen YW, Kang ET, Neoh KG, Grener A: **Preparation of hollow silica nanospheres by surface-initiated atom transfer radical polymerization on polymer latex templates.** *Adv Funct Mater* 2005, **15**(1):113–117.
9. Darbandi M, Thomann R, Nann T: **Silica coated nanocomposites.** *Chem Mater* 2007, **19**(7):1700–1703.
10. Deng ZW, Chen M, Zhou S, You B, Wu LM: **A novel method for the fabrication of monodisperse hollow silica spheres.** *Langmuir* 2006, **22:**6403–6407.
11. Chen M, Wu L, Zhou S, You B: **A method for the fabrication of monodisperse hollow silica spheres.** *Adv Mater* 2006, **18:**801–805.
12. Tsai MS, Li MJJ: **A novel process to prepare a hollow silica sphere via chitosan-polyacrylic acid (CS-PAA) template.** *Non-Cryst Solids* 2006, **352**(26–27):2829–2833.
13. Botterhuis NE, Sun QY, Magusin PCMM, Van Santen RA, Sommerdijk NA: **Hollow silica spheres with an ordered pore structure and their application in controlled release studies.** *Chem-Eur J* 2006, **12**(5):1448–1456.
14. Han YS, Jeong GY, Lee SY, Kim HKJ: **Hematite template route to hollow-type silica spheres.** *Solid State Chem* 2007, **180:**2978–2985.
15. Wan Y, Yu SHJ: **Polyelectrolyte controlled large-scale synthesis of hollow silica spheres with tunable sizes and wall thicknesses.** *Phys Chem C* 2008, **112**(10):3641–3647.
16. Chen Y, Chen HR, Guo LM, He QJ, Chen F, Zhou J, Feng JW, Shi JL: **Hollow/rattle-type mesoporous nanostructures by a structural difference-based selective etching strategy.** *ACS Nano* 2010, **4:**529–539.
17. Lou XW, Archer LA, Yang ZC: **Hollow micro-/nanostructures: synthesis and applications.** *Adv Mater* 2008, **20:**3987–4019.
18. Ding SJ, Chen JS, Qi G, Duan X, Wang Z, Giannelis EP, Archer LA, Lou XWJ: **Formation of SnO_2 hollow spheres inside silica nanoreactors.** *Am Chem Soc* 2011, **133:**21–23.

19. Zhang Q, Ge JP, Goebl J, Hu YX, Lu ZD, Yin YD: **Rattle-type silica colloidal particles prepared by a surface-protected etching process.** *Nano Res* 2009, **2:**583–591.
20. Tan LF, Chen D, Liu HY, Tang FQ: **A silica nanorattle with a mesoporous shell: an ideal nanoreactor for the preparation of tunable gold cores.** *Adv Mater* 2010, **22:**4885–4889.
21. Sanles-Sobrido M, Exner W, Rodríguez-Lorenzo L, Rodríguez-Gonzalez B, Correa-Duarte MA, Alvarez-Puebla RA, Liz-Marzan LM: **Design of SERS-encoded, submicron, hollow particles through confined growth of encapsulated metal nanoparticles.** *J Am Chem Soc* 2009, **131:**2699–2705.
22. Li LL, Tang FQ, Liu HY, Liu TL, Hao NJ, Chen D, Teng X, He JQ: **In vivo delivery of silica nanorattle encapsulated docetaxel for liver cancer therapy with low toxicity and high efficacy.** *ACS Nano* 2010, **4:**6874–6882.
23. Ren N, Wang B, Yang YH, Zhang YH, Yang WL, Yue YH, Gao Z, Tang Y: **General method for the fabrication of hollow microcapsules with adjustable shell compositions.** *Chem Mater* 2005, **17:**2582–2587.
24. Yamada Y, Mizutani M, Nakamura T, Yano K: **Mesoporous microcapsules with decorated inner surface: fabrication and photocatalytic activity.** *Chem Mater* 2010, **22:**1695–1703.
25. Zhang Q, Zhang TR, Ge JP, Yin YD: **Permeable silica shell through surface-protected etching.** *Nano Lett* 2008, **8:**2867–2871.
26. Cao S, Fang L, Zhao Z, Ge Y, Piletsky S, Anthony P, Turner F: **Hierachically structured hollow silica spheres for high efficiency immobilization of enzymes.** *Adv Funct Mater* 2013, **23**(17):2162–2167.
27. Zhang TR, Ge JP, Hu YX, Zhang Q, Aloni S, Yin YD: **Formation of hollow silica colloids through a spontaneous dissolution–regrowth process.** *Angew Chem Int Ed* 2008, **47:**5806–5811.
28. Zhang TR, Zhang Q, Ge JP, Goebl J, Sun MW, Yan YS, Liu YS, Chang CL, Guo JH, Yin YDJ: **A self-templated route to hollow silica microspheres.** *Phys Chem C* 2009, **113:**3168–3175.
29. Yang ZZ, Niu ZW, Lu YF, Hu Z, Han Charles C: **Templated synthesis of inorganic hollow spheres with a tunable cavity size onto core–shell gel particles.** *Angew Chem Int Ed* 2003, **115:**1987–1989.
30. Zhong Z, Yin Y, Gates B, Xia Y: **Preparation of mesoscale hollow spheres of TiO_2 and SnO_2 by templating against crystalline arrays of polystyrene beads.** *Adv Mater* 2000, **12:**206–209.
31. Wang X, Miao X-R, Li Z-M, Deng W-L: **Fabrication of microporous hollow silica spheres templated by NP-10 micelles without calcinations.** *Appl Surf Sci* 2011, **257:**2481–2488.
32. Okubo M, Ito A, Kanenobu T: **Production of submicron-sized multihollow polymer particles by alkali/cooling method.** *Colloid Polym Sci* 1996, **274:**801–804.
33. Li W, Sha X, Dong W, Wang Z: **Synthesis of stable hollow silica microspheres with mesoporous shell in nonionic W/O emulsion.** *Chem Commun* 2002, **20:**2434–2435.
34. Zi-Wei D, Min C, Shu-Xue Z, Bo Y, Li-Min W: **A facile approach for the fabrication of monodisperse hollow silica spheres.** *Chem J Chin U* 2006, **27**(10):1795–1799.
35. Wu XF, Tian YJ, Cui YB, Wei LQ, Wang Q, Chen YF: **Raspberry-like silica hollow spheres: hierarchical structures by dual latex-surfactant templating route.** *J Phys Chem C* 2007, **111:**9704–9708.
36. Lou X, Schumacher T, Yang H, Ding A: **Synthesis and characterisation of silica–polymer hybrid core–shell and hollow spheres for drug delivery.** *J Control Release* 2011, **152:**e1–e132.
37. Stober W, Fink A, Bohn EJ: **Controlled growth of monodisperse silica spheres in the micron size range.** *Colloid Interface Sci* 1968, **26:**62–69.
38. Wang W, Gu BH, Liang LY, Hamilton WJ: **Fabrication of two- and three-dimensional silica nanocolloidal particle arrays.** *Phys Chem B* 2003, **107:**3400–3404.
39. Lu LH, Capek R, Kornowski A, Gaponik N, Eychmuller A: **Selective fabrication of ordered bimetallic nanostructures with hierarchical porosity.** *Angew Chem Int Ed* 2005, **44:**5997–6001.
40. Blasse G, Grabmaier BC: *How does a luminescent material absorb its excitation energy? Luminescence Materials.* New York: Springer; 1994:22.
41. Shionoya S, Yen WM: *Principal phosphor materials and their optical properties. Phosphor Handbook.* Boca Raton: CRC Press; 1999:190.
42. Mho S-I, Wright JC: **Site selective spectroscopy of defect chemistry in CdF_2:Eu.** *J Chem Phys* 1982, **77:**1183.
43. Judd BR: **Optical absorption intensities of rare-earth ions.** *Phys Rev* 1962, **127:**750.
44. Ofelt GS: **Intensities of crystal spectra of rare-earth ions.** *J Chem Phys* 1962, **37:**511.
45. Zeng HC: **Ostwald ripening: a synthetic approach for hollow nanomaterials.** *Curr Nanosci* 2007, **3:**177–181.
46. Zhang H, Zhao Y, Daniel L, Akins J: **Synthesis and new structure shaping mechanism of silica particles formed at high pH.** *J Solid State Chem* 2012, **194:**277–281.
47. Zhu H, Yang D, Zhu L, Li D, Chen P, Yu G: **Hydrothermal synthesis and photoluminescence properties of $La_{2-x}Eu_xSn_2O_7$ ($x = 0$–2.0) nanocrystals.** *J Am Ceram Soc* 2007, **90:**3095.
48. Yuan J, Wang Z: **A facile method of synthesis of asymmetric hollow silica spheres.** *J Colloid Interface Sci* 2011, **362:**15–20.
49. Ma M-Y, Zhu Y-J, Li L, Cao S-W: **Nanostructured porous hollow ellipsoidal capsules of hydroxyapatite and calcium silicate: preparation and application in drug delivery.** *J Mater Chem* 2008, **18:**2722–2727.
50. Abbas A, Borujeni AA, Najafi M, Hajian A: **Synthesis and characterization of supported silica nano hollow spheres with CdS quantum dots.** *J Mol Liq* 2012, **174:**124–128.
51. Chen D, Li LL, Tang FQ, Qi S: **Facile and scalable synthesis of tailored silica "nanorattle" structures.** *Adv Mater* 2009, **21:**3804–3807.
52. Yu Q, Wang P, Hu S, Hui J, Zhuang J, Wang X: **Hydrothermal synthesis of hollow silica spheres under acidic conditions.** *Langmuir* 2011, **27:**7185–7191.
53. Zhu Y, Fang Y, Borchardt L, Kaskel S: **PEGylated hollow mesoporous silica nanoparticles as potential drug delivery.** *Micropor Mesopor Mat* 2011, **141:**199–206.

doi:10.1186/1556-276X-8-435
Cite this article as: Li *et al.*: A facile approach to synthesize SiO_2 · Re_2O_3 (Re = Y, Eu, La, Sm, Tb, Pr) hollow sphere and its application in drug release. *Nanoscale Research Letters* 2013 **8**:435.